Journal of ELECTRONIC MATERIALS, Vol. 49, No. 2, 2020
https://doi.org/10.1007/s11664-019-07656-y

Effect of Simultaneous Replacement of Fe with Zr and Ni in a Mechanically Alloyed Multicomponent Fe-Based Amorphous Alloy

ZAHRA ALLAFE RAZZAGHI,[1] ABBAS KIANVASH,[1,2] and ABOLFAZL TUTUNCHI[1]

1.—Institute of Mechanical Engineering, Department of Materials Engineering, University of Tabriz, Tabriz 51666-16471, Iran. 2.—e-mail: akianvash@tabrizu.ac.ir

In this study, Fe-based amorphous powder with a composition of $Fe_{40}Ni_{25}Zr_{10}Si_{10}B_{15}$ (compound Q) was prepared by a partial replacement of Fe with Zr and Ni in a $Fe_{75}Si_{10}B_{15}$ (compound P) via a mechanical alloying route. This substitution led to a decrease in amorphization time and consequently a significant improvement in thermal stability. The structure and thermal properties of the prepared powders were investigated by x-ray diffraction (XRD) pattern and differential scanning calorimetry (DSC), respectively. XRD and DSC results revealed that complete amorphization is achieved after 50 h of milling and glass forming ability width (ΔT_x) increases from 50°C to 66°C by substitution of Fe with Zr and Ni in compound P. Magnetic properties of the samples, investigated by vibrating sample magnetometry, indicated that in spite of a negligible decrease in saturation magnetization (M_s) by Fe replacement with Zr and Ni, the coercivity (H_c) shows a positive response to this change as a soft magnetic material, decreasing from 35 Oe to 15 Oe.

Key words: Iron-based bulk metallic glasses, mechanical alloying, saturation magnetization, coercivity, soft magnetic materials

INTRODUCTION

In the past two decades, considerable attention has been devoted to the Fe-based bulk metallic glasses due to their superior soft magnetic properties combined with excellent mechanical properties in comparison with conventional crystalline steels.[1–5] Furthermore, Fe-based systems are significantly inexpensive in comparison to other bulk metallic glasses investigated so far (for example, those based on Pd,[6] Au,[7] Zr,[8] Hf,[9] etc.). There are a number of alternative techniques for producing Fe-based glassy alloys in powder shape, such as rapid solidification,[10] gas or water atomization,[11,12] mechanical alloying and so on. However, mechanical alloying, as reported by a number of investigators,[13,14] is the most widely used route for producing these materials. Mechanical alloying has a number of advantages such as low equipment cost, facility of processing and the possibility of massive production.[15,16] Furthermore, it is well-known that the amorphous alloys are usually obtained in a chemical composition close to the deep eutectic point and negative heat mixing in rapid solidification or atomizing methods, but in mechanical alloying it is possible to produce amorphous materials in compositions far from the eutectic points, with even positive heat mixing.[17,18]

Despite the relatively high saturation magnetization, the application of Fe-based alloys, as soft magnetic materials, have been limited; this is mainly because of their low glass forming abilities (GFA). Therefore, in recent years, tremendous efforts have been devoted to create amorphous metallic alloys with high GFA and thus high thermal stabilities.[19,20] It has been proved that the

(Received January 14, 2019; accepted September 17, 2019; published online November 26, 2019)

addition of small amounts of some elements such as P ameliorates the GFA due to the enhancement of the negative mixing enthalpy. Furthermore, this element leads to an increase in atomic size mismatches among constituent elements. Effect of Nb addition is as the same as the addition of P; however, it has one more effect which is decreasing the quantity of oxygen helping the improvement of thermal stability. Mo alloying with Fe based amorphous alloys results in improving GFA according to the reduction of the liquidus temperature and inhibiting from crystalline phases formation.[21–24]

The goal of the present research is to represent a new class of amorphous metallic alloys from Fe–Si–B based mixture via mechanical alloying technique. The simultaneous substitution of small quantities of Ni and Zr in this compound, is considered in order to decrease the required milling time for achieving the amorphous state, which is followed by enhancing the alloys' GFA. These additive elements are selected on the basis of obtaining higher intermetallic phases which could be formed between Zr and Ni under equilibrium conditions, and higher negative heat of formation between Zr and other elements.[25–27]

EXPERIMENTAL

Amorphous powders with nominal compositions of $Fe_{75}Si_{10}B_{15}$ (P) and $Fe_{40}Ni_{25}Zr_{10}Si_{10}B_{15}$ (Q) were prepared via a mechanical alloying route. Mixtures of pure Fe, Ni, Zr and Si, all with a purity of 99.9% and B, with a purity of 99.5% in the form of powders, supplied by Alfa Aesar, were mixed together and ground in a medium energy planetary ball mill with a rotation speed of 350 rpm. The ball-powder ratio (BPR) was 12:1. The milling balls and chambers were made of a hardened and tempered alloy steel. To prevent oxidation, the milling was carried out under pure argon atmosphere and a gloves box was used for sample handling. The structural and phase evolution of the samples was accomplished by use of a D8 advance x-ray diffraction (XRD) (Bruker, Germany) with Cu Kα radiation (λ = 1.5406 Å). Scanned angular interval was 2θ = 10–90°. The thermal investigation of the amorphous powders was carried out using a NETZSCH differential scanning calorimetry (DSC). The analyzed temperature range was 20–700°C with a heating rate of 0.67 K/s under an Ar atmosphere. In order to study the morphology of the powder, scanning electron microscopy (SEM) (TESCAN MIRA3-FEG) was used. The saturation magnetization (M_s) and coercive force (H_c) of the powders were determined by a vibrating sample magnetometer (VSM) (MDK) with a maximum applied field of 800 kA/m at ambient temperature.

RESULTS AND DISCUSSION

Figures 1 and 2 show the XRD patterns for alloy P and Q at different milling times, respectively. The Bragg reflections in the starting sample patterns,

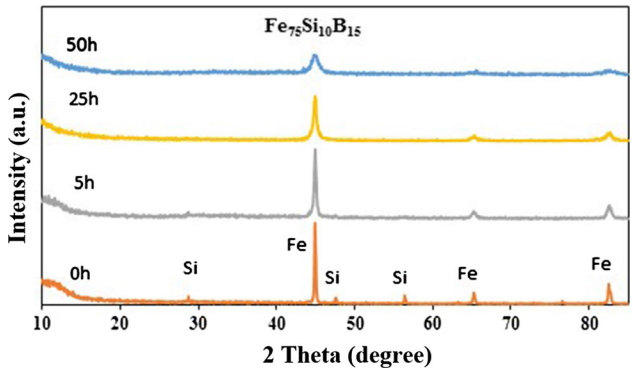

Fig. 1. XRD patterns for elemental mixture of Fe–Si-B powders (0 h) and $Fe_{75}Si_{10}B_{15}$ powders milled for different milling times of 5-50 h.

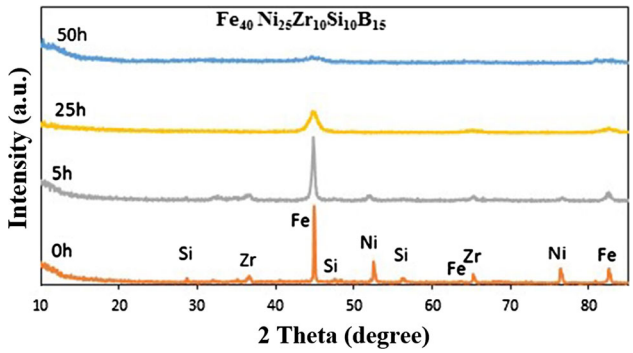

Fig. 2. XRD patterns for elemental mixture of Fe–Si-B-Zr–Ni powders (0 h) and $Fe_{40}Ni_{25}Zr_{10}Si_{10}B_{15}$ powders milled for different milling times of 5-50 h.

are related to elemental Fe, Si, Ni and Zr. The Bragg reflections due to B cannot be observed in these mixtures which could be related to its small content, or due to its low x-ray scattering factor and amorphous state. After 50 h of milling, alloy Q in the form of powder did not show any diffraction peak(s) due to crystalline phase(s). However, the corresponding XRD pattern for alloy P illustrated some minor Bragg peaks which suggests that, even after 50 h of milling, the fully amorphous condition was not achieved in this sample.

Reduction of required milling time to achieve fully amorphous condition in compound Q in comparison to P, could be related to formation of extra intermetallic phase(s) due to presence of Ni and Zr in this compound, as well as the reduction in heat of formation of Zr-intermetallic(s) with other elements.[25]

SEM micrographs of the 50-h-milled powders of P and Q are presented in Fig. 3a and b, respectively. The powder particles were found to be agglomerated in both compounds having polyhedral irregular shapes which is a general characteristic of mechanical alloying. The average particle size in powder Q was found to be relatively smaller than that of powder P (Fig. 3); this could be attributed to higher degree of amorphization in compound Q.[15] For

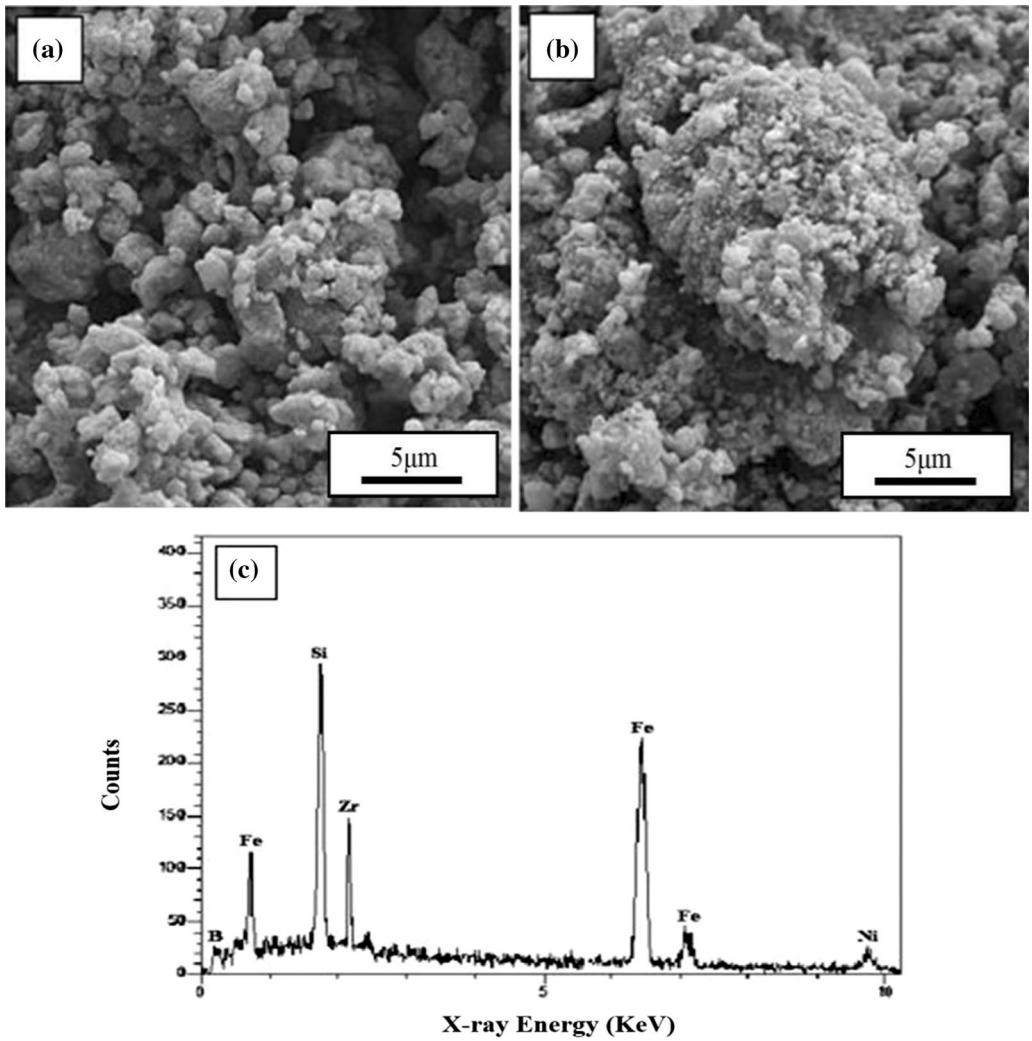

Fig. 3. SEM images of 50 h-milled powders of (a) P and (b) Q, and (c) EDS spectrum of Q.

investigation of oxidation probability, EDS analysis was carried out (Fig. 3c). According to this figure, no peak(s) of oxygen was obtained which shows that the powder was not oxidized.

The corresponding particle size distributions for powders P and Q are shown in Fig. 4a and b, respectively. The Gaussian like profile is revealed in both particle size distributions, which is related to balance between cold welding and fracturing phenomena during the milling. The average powder particle size in powder P is almost in the range of micro ($\sim$ 421 nm), however, by partial substitution of Fe with Zr and Ni in compound Q, the average particle size decreases to $\sim$ 112 nm; these are in good agreements with SEM results.

To demonstrate the correlation between milling time and glass forming ability (GFA) of amorphous powders, the thermal stability of the powder samples was examined using DSC scans. Figure 5 exhibits the DSC traces for initial elemental mixer of powders and the mixed powders after 50 h of milling. The crystalline structure in the initial elemental mixture of powders was proved by the DSC curve (Fig. 5a) due to rather a straight graph during heating. The existence of broad exothermic peaks at the range of 90–170°C in both the P (Fig. 5b) and Q (Fig. 5c) powders are related to removal of stresses, induced in the powders by milling.[28] The large and broad exothermic peak (the second peak) at the temperature range of 480–540°C in Fig. 4b, could be due to primary crystallization of amorphous powder.[13] The exothermic peak in Q amorphous powder (Fig. 4c), seems to be more broadened by comparison with that of P powder. This could mean that there is a higher volume fraction of the amorphous phase in compound Q in comparison to compound P. The glass transition (T_g) and the crystallization temperatures (T_x) are also presented in Fig. 5b and c. Both the T_g and T_x temperatures have respectively increased from 443°C to 482°C and from 493°C to 548°C by replacing Fe with Ni and Zr. The super cooled liquid region, ΔT_x ($T_x - T_g$), is severely correlated to GFA of the samples. Enhancements in ΔT_x (from 50°C to

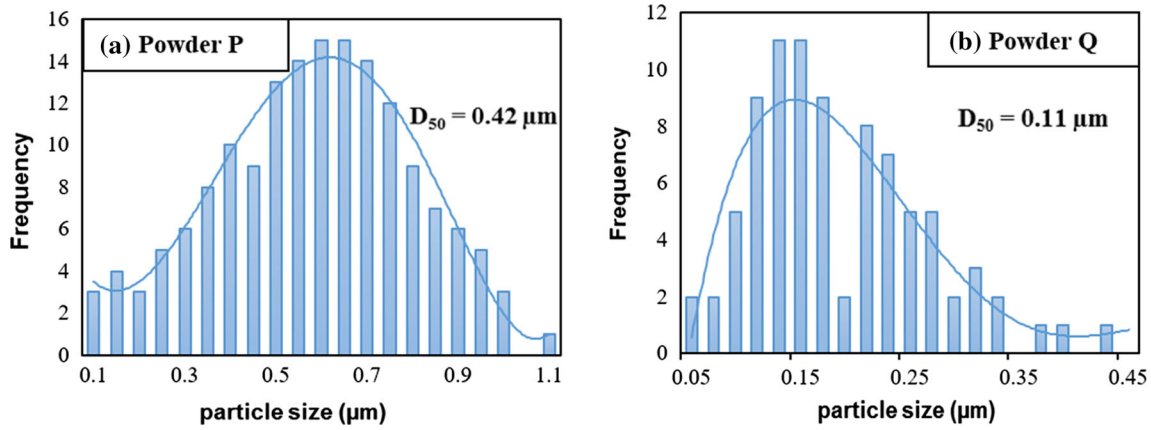

Fig. 4. The particle size distributions in the 50 h ball-milled powders of: (a) P and (b) Q.

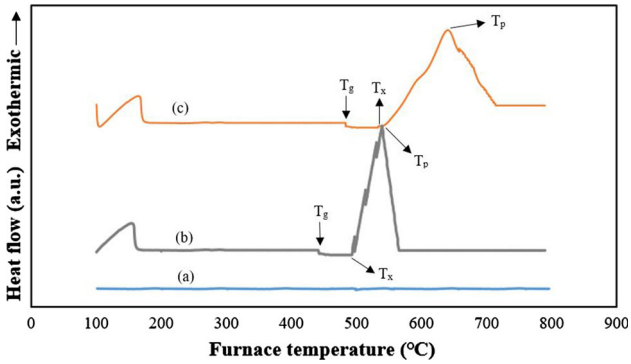

Fig. 5. DSC heating curves of (a) starting elemental mixture of powders, (b) 50-h-milled $Fe_{75}Si_{10}B_{15}$ and (c) 50-h-milled $Fe_{40}Ni_{25}Zr_{10}Si_{10}B_{15}$ powders.

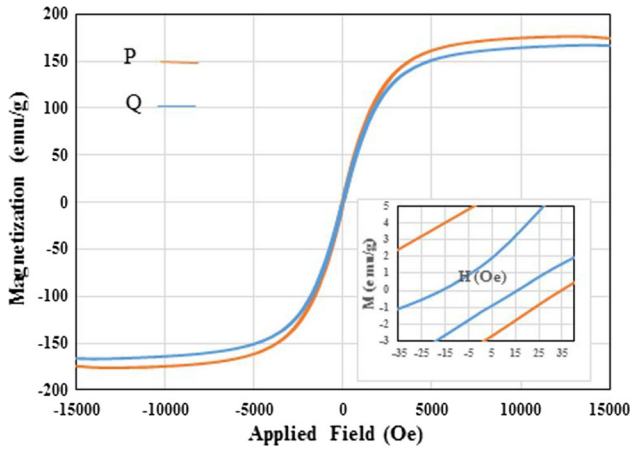

Fig. 6. M-H hysteresis loops for 50-h-milled amorphous powders P and Q.

66°C) and T_x (from 493°C to 548°C), by partial replacement of Fe in compound P with Zr and Ni (compound B), causes an enhancement of thermal stability in the latter. The large ΔT_x of alloy Q is related to the larger atomic radius of Zr (1.602 Å) in comparison to that of Fe (1.26 Å) and high heat of mixing between Zr and Ni that lead to denser random-packed structures. Under these circumstances, atomic rearrangement requires higher energy for crystallization and, consequently, the thermal stability of the amorphous phase is enhanced.[20] Thus, there is a good correlation between the milling time and thermal stability of powders which are proved by XRD and DSC results.

The room temperature *M–H* hysteresis loops of amorphous powders P and Q are presented in Fig. 6. The M_s value decreases slightly from 178 emu/g to 167 emu/g by substituting Fe with Zr and Ni. This is clearly related to higher M_s value of Fe (217.6 emu/g) in comparison to Ni (55.1 emu/g) and Zr (which is essentially paramagnetic).[29] However, the M_s value in the present amorphous powder was still higher than that of the previous amorphous Fe magnetic powder.[11] Regarding the H_c, it is well known that the coercivity of the as-milled powder is relatively higher than those of the powders produced by other methods due to a higher level of the internal stresses induced by milling.[30] However, in the present study, H_c value decreased significantly from 35 Oe in powder P to 15 Oe in powder Q; this is related to a partial disordered magnetic structure which could be induced by interatomic distance enhancement between Fe atoms, by partial substitution of Fe with Zr and Ni atoms, as well as due to development of a fully amorphous phase in powder Q after 50 h milling.

CONCLUSION

By partial replacement of Fe with Ni and Zr in ternary $Fe_{75}Si_{10}B_{15}$ (P) powder, the amorphous quinary $Fe_{40}Ni_{25}Zr_{10}Si_{10}B_{15}$ (Q) powder was successfully produced using the mechanical alloying route. A fully amorphous powder was produced after 50 h of milling in powder Q, while minor Bragg peaks were observed in the XRD pattern of 50 h milled for powder P. The DSC results showed that the super cooled liquid region is significantly increased by substitution of Fe with Zr and Ni; this

is related to the larger atomic radius of Zr (1.602 Å) by comparison with Fe (1.26 Å), and higher heat of mixing between Zr and Ni. The XRD and DSC results demonstrated the superb correlation between milling time and GFA of amorphous Fe based powders which was the main purpose in this paper. Moreover, reasonably higher M_s value of 167 emu/g and relatively lower H_c of 15 Oe, in comparison to other mechanically alloyed Fe-based powders, have been detected by replacing of Fe in the present compound. Therefore, the present powder could be used as a functional magnetic material due to its valuable magnetic behavior.

REFERENCES

1. R. Babilas and R. Nowosielski, *Arch. Mater. Sci. Eng.* 44, 5 (2010).
2. T.R. Anantharaman, *Metallic Glasses: Production, Properties and Applications* (Zurich: Trans Tech Publ, 1984).
3. A. Inoue, *Acta Mater.* 48, 279 (2000).
4. A. Inoue, B. Shen, and C. Chang, *Intermetallics* 14, 936 (2006).
5. F. Wang, A. Inoue, F.L. Kong, S.L. Zhu, E. Shalaan, F. Al-Marzouki, W.J. Botta, C.S. Kiminami, Y.P. Ivanov, and A.L. Greer, *Acta Mater* 170, 50–61 (2019).
6. A. Inoue, N. Nishiyama, and H. Kimura, *Mater. Trans. JIM* 38, 179 (1997).
7. J. Schroers, B. Lohwongwatana, and W.L. Johnson, *Appl. Phys. Lett.* 87, 061912 (2005).
8. A. Inoue, T. Zhang, and T. Masumoto, *Mater. Trans. JIM* 31, 177 (1990).
9. X. Gu, L. Xing, and T. Hufnagel, *J. Non-Cryst. Solids* 311, 77 (2002).
10. D. Zhang, *Prog. Mater Sci.* 49, 537 (2004).
11. Y.B. Kim, D.H. Jang, H.K. Seok, and K.Y. Kim, *Mater. Sci. Eng. A* 449, 389 (2007).
12. J. Guo, Y. Dong, Q. Man, Q. Li, C. Chang, and X.M. Wang, *J. Magn. Magn. Mater.* 401, 432 (2016).
13. B. Neamtu, H.F. Chicinaş, T.F. Marinca, and O. Isnard, *Mater. Chem. Phys.* 183, 83 (2016).
14. B. Murty and S. Ranganathan, *Int. Mater. Rev.* 43, 101 (1998).
15. A. Hajalilou, M. Hashim, and R. Ebrahimi-Kahrizsangi, *J. Alloys Compd.* 633, 306 (2015).
16. R.A. Sekhar, S. Samal, N. Nayan, and S.R. Bakshi, *J. Alloys Compd* 787, 123 (2019).
17. C. Suryanarayana, *Prog. Mater Sci.* 46, 1 (2001).
18. C. Suryanarayana, *Mechanical Alloying and Milling* (New York: Marcel Dekker, 2004).
19. C. Suryanarayana and A. Inoue, *Int. Mater. Rev.* 58, 131 (2013).
20. Y. Lv, Q. Chen, and Y. Huang, *J. Rare Earth* 37, 4 (2019).
21. Z. Lu and C. Liu, *J. Mater. Sci.* 39, 3965 (2004).
22. K.R. Zhu, W. Jiang, J.L. Wu, and B. Zhang, *Int. J. Min. Met. Mater. Mater.* 24, 8 (2017).
23. Z. Li, S. Zhou, G. Zhang, and W. Zheng, *Materials* 11, 7 (2018).
24. C.G. Jia, J. Pang, S.P. Pan, Y.J. Zhang, K.B. Kim, J.Y. Qin, and W.M. Wang, *Corros. Sci.* 147, 94 (2019).
25. S. Sharma, R. Vaidyanathan, and C. Suryanarayana, *Appl. Phys. Lett.* 90, 111915 (2007).
26. R.G. Adli, A. Kianvash, M.G. Hosseini, A. Hajalilou, and E. Abouzari-Lotf, *Ceram. Int.* 44, 16 (2018).
27. R.G. Adli, A. Kianvash, M.G. Hosseini, A. Hajalilou, and E. Abouzari-Lotf, *JOM* 1, 2 (2019). https://doi.org/10.1007/s11837-03486-9.
28. B. Neamtu, T.F. Marinca, I. Chicinaş, and O. Isnard, *J. Alloys Compd.* 600, 1 (2014).
29. R. Babilas, A. Radoń, and P. Gębara, *Acta Phys. Pol. A.* 131, 726 (2017).
30. A. Taghvaei, F. Ghajari, and D. Markó, *J. Magn. Magn. Mater.* 395, 354 (2015).